

A two-phase flow model of wave-induced sheet flow

Modèle diphasique d'un écoulement cisailé ondulatoire

TAI-WEN HSU, *Professor, Department of Hydraulic and Ocean Engineering, National Cheng Kung University, Tainan 701, Taiwan*

HSIEN-KUO CHANG, *Associate Professor, Department of Civil Engineering, National Chiao Tung University, Hsin Chu 300, Taiwan*

CHIH-MIN HSIEH, *Ph.D. Student, Department of Hydraulic and Ocean Engineering, National Cheng Kung University, Tainan 701, Taiwan*

ABSTRACT

This paper presents a two-phase flow model that simulates the fluid and sediment motions in the sheet flow region under oscillatory conditions. Some major forcing terms such as the fluid/particle and particle/particle interactions and turbulent stresses are included in the model. By improving some assumptions of most existing models, the present model specifies the equivalent sand roughness and bed concentration as a function of the Shields parameter, which is variable with time and is physically more realistic over a mobile flat bed. A wave friction factor, which is governed by a new parameter, is obtained from the present model formulation. The present model is shown to provide a more accurate estimate of sediment concentrations than those models using a constant equivalent sand roughness. Numerical analyses also show that the suspended sediment retards the mean velocity and suppresses turbulence.

RÉSUMÉ

Cet article présente un modèle d'écoulement diphasique qui simule les mouvements de fluide et de sédiment dans la région d'écoulement cisailé en présence de conditions oscillantes. Certains termes sources prépondérants tels que les interactions fluide/particule et particule/particule ainsi que les contraintes turbulentes sont inclus dans le modèle. Pour améliorer les hypothèses de la plupart des modèles existants, ce modèle définit une rugosité du sable et une concentration de lit équivalentes en fonction du paramètre de Shields, qui est variable en temps et est physiquement plus réaliste au-dessus d'un lit plat mobile. Un facteur de frottement d'onde, régi par un nouveau paramètre, est obtenu à partir de la formulation du modèle. On montre que le présent modèle fournit une évaluation plus précise des concentrations en sédiment que les modèles qui utilisent une rugosité équivalente de sable constante. Les analyses numériques montrent également que le sédiment en suspension freine la vitesse moyenne et supprime la turbulence.

Keywords: Sheet flow; $k-\epsilon$ model; sediment concentration; wave friction factor.

1 Introduction

When water waves propagate from a deep water to a shallow water sandy zone, the lower layer of the flow usually become turbulent. A sheet flow is formed, when the fluid motion is in a sweep condition. Sand ripples are not present and sand moves in a thin layer. The sheet flow condition is identified as the most important transport mode due to the large sediment transport rate. This condition is not normally present, but probably takes place more frequently under some storm conditions, resulting in significant changes to a beach.

The Shields parameter is normally used to measure flow intensity in the sediment-laden flow, which is defined by

$$Y = \frac{\tau_b}{(\rho_s - \rho_f)gD_{50}} \quad (1)$$

where τ_b is the bottom shear stress, ρ_s density of sand, ρ_f density of fluid, g the gravitational acceleration, and D_{50} the medium diameter of sand grains. Wilson's (1989b) experimental findings show that the wave-induced sheet flow occurs when the Shields parameter exceeds than 0.8. In Eq. (1), the bottom shear stress is defined as

$$\frac{\tau_b}{\rho_f} = C_f |U|U \quad (2)$$

where C_f is the wave friction factor and U is the free stream velocity. For an oscillatory flow, the free stream velocity is given by

$$U = U_m \sin \omega t \quad (3)$$

where $U_m = A_b \omega$ is the amplitude of the free stream velocity, A_b the excursion of water particle at bottom, $\omega = 2\pi/T$ the angular frequency and T the wave period.

The key feature of the wave-induced sheet flow is the mixture of turbulent flow and suspended sediments, i.e. a two-phase flow. When sediments are suspended by an oscillatory flow, the vertical gradient of the sediment concentration varies accordingly. This may cause the velocity profile to deviate appreciably from that without suspended sediment, and it in turn changes the flow resistance and produces a different sediment concentration distribution. Quantification of the interaction between fluid and sediment is essential in determining the sediment transport in coastal engineering practice.

Effects of suspended sediments on the velocity profile in the two-phase flow have been studied by many researchers (e.g. Vanoni, 1946; Einstein and Chien, 1955). Their observations were interpreted by a contemporary boundary layer theory with a decrease in von Karman's constant κ . Coleman (1980) re-examined the effects, by fitting the velocity profiles with and without suspended sediments, and concluded that the sediment suspension does not alter the value of κ from its usual value of 0.4. Other developments (Smith and McLean, 1977; Adams and Weatherly, 1981; Kobayashi and Seo, 1985; Hsu and Ou, 1994) used a theory of stably stratified boundary layer flows to explain the effects in a more realistic manner, without recourse to κ . In these models, both the diffusion coefficient and eddy viscosity are expressed as functions of the gradient Richardson number.

Recently, numerical simulations of the two-phase flow have received much attention. A turbulence model allows a more accurate description of the two-phase flow. It may be possible to obtain better results with the use of a numerical model. In this paper, a complete two-phase flow model is presented for the simulation of flow kinematics, turbulence dynamics and sediment motions under sheet flow conditions. The numerical predictions are compared with the experimental measurements to confirm the validity of the model.

2 Review of numerical models of the two-phase flows

Most models for predicting sediment transport are based on a single-phase flow approach. Bakker (1974) developed a numerical model to calculate suspended sediment concentration, in which the diffusion coefficient obeys Prandtl's mixing length hypothesis. Fredsoe *et al.* (1985) introduced a mathematical model to describe both the instantaneous and mean sediment concentrations profiles by assuming a diffusion coefficient that varies parabolically from sea bottom. Hagatun and Eidsvik (1986) presented a turbulence model to simulate the instantaneous sediment concentration and the turbulent boundary layer in the sheet flow regime over a flat bed. Ahilan and Sleath (1987) investigated the motion of sediment in oscillatory flow over a flat bed both theoretically and experimentally. Nadaoka and Yagi (1990) developed a mobile bed model considering the mass and momentum transport of a single-phase flow. Ribberink and Al-Salem (1995) conducted time-dependent measurements of flow velocities and sediment concentrations in a large oscillating water tunnel. They also applied a simple model based on a Prandtl's

mixing length turbulence closure to predict flow velocities and sediment concentrations. The fluid/particle and particle/particle interactions are not accounted for in these models. Thus, the single-phase flow models have their limitation in solving sediment motions with the relatively high sediment concentration that usually happens under sheet flow conditions.

In recent years, several two-phase flow modeling techniques have been developed. Extending Kobayashi and Seo's (1985) work, Asano (1990) proposed a partial two-phase flow model in which the vertical velocity of particles was approximated by an empirical expression rather than being solved in the governing equations. Another partial two-phase flow model was reported by Ono *et al.* (1996), in which the horizontal velocities of fluid and particles were assumed to be the same. This model is applicable to various modes of transport over flat and ripple beds. Due to some simplifications, these models do not provide as much insight into the mechanism of fluid/particle interaction as a complete two-phase flow modeling approach. Li and Sawamoto (1995) followed Asano's work by formulating a complete set of two-phase flow equations. However, they were unable to obtain stable solutions for sand transport cases due to the deficiency in the numerical schemes and their predictions of sediment concentration are unsatisfactory compared with experimental measurements. Gotoh and Sakai (1997) presented a numerical simulation of the sediment transport and flow kinematics with a closure for particle/particle interactions in the sheet flow regime. The mechanism affecting the velocity profile of the sediment particles is clarified from the viewpoint of the granular material dynamics, but the fluid/particle interaction is simplified in the model. Dong and Zhang (1999) proposed a complete two-phase flow model that simulates the fluid and sediment motions in the sheet flow regime under oscillatory flow conditions. All major forcing terms such as the fluid/particle and particle/particle interactions and the turbulent stresses are included in the model. Their models are based on the assumption of an eddy viscosity model which is too restrictive to predict this relatively complicated flow. A review by Justesen (1988) reveals that in order to predict the complicated flow, the minimum requirement of the closure is a two-equation model of turbulence (or referred to as a $k-\epsilon$ model).

It is known that one of the major sources of ambiguity in the modeling of the two-phase flow stems from the definition of the computational bottom boundary, along with the conditions of velocity, concentration and other flow quantities that must be specified on it. Although most existing two-phase flow models appear to reproduce the experimental data well, their choice of a constant equivalent sand roughness as the bottom boundary conditions is physically unrealistic. It has been estimated by the theories and experiments (Grant and Madsen, 1982; Wilson, 1989a,b; Wilson *et al.*, 1995) that the mobile equivalent sand roughness k_s of the boundary layer is not proportional to the particles size, but rather the thickness of the sediment moving layer in the bed load region. Grand and Madsen (1982) reported that the mobile sand roughness k_s varies with the Shields parameter, and the height and length of sand ripple. Wilson (1989a) proposed a value of the dimensionless roughness k_s/D_{50} for a moving bed,

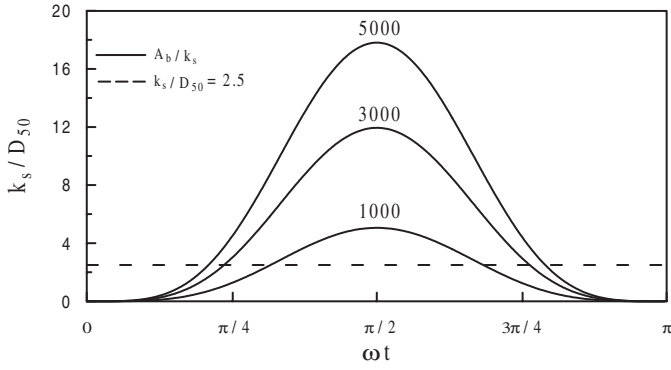


Figure 1 Phase variations of equivalent sand roughness for different values of the relative roughness A_b/k_s in two-phase flow.

which is proportional to the Shields parameter Y , i.e.

$$\frac{k_s}{D_{50}} = 5Y \quad (4)$$

where k_s is the equivalent sand roughness in the two-phase flow. Figure 1 shows a typical example of phase variations of a mobile equivalent sand roughness for different values of the relative roughness A_b/k_s . A conventional relation of $k_s/D_{50} = 2.5$ (Einstein and Chien, 1955) is also plotted for comparison. It is noted that the value of k_s/D_{50} increases with the increase of A_b/k_s . On the other hand, the bed sediment concentration is usually specified as a constant value ($c_b = c_m = 0.65$, where c_b is the bed concentration and c_m is the maximum concentration) at the bottom boundary in the two-phase models (Ono *et al.*, 1966; Dong and Zhang, 1999). This assumption is too simplified to describe the complex flow. According to the analysis of Engelund and Fredsoe (1976), the bed concentration is not constant, but is related to the Shields parameter.

Wilson (1989b) applied Eq. (4) to estimate the wave friction factor by assuming a logarithmic velocity profile. His results show that the wave friction factor depends on a dimensionless parameter, relating to the relative roughness and the wave steepness. He extended this approach to deal with asymmetric and irregular waves, and obtained relationship for the wave friction factor and the transition from bed forms to sheet flow. However, Vongvisessomjai (1986) showed that the logarithmic profile in experimental data is only valid for flow close to the bottom. Far away from the bottom, the logarithmic profile overestimates the mean velocity. Following the approach of Wilson (1989b), Hsu and Ou (1994) presented a single-phase flow model to describe mean sediment concentration and turbulent boundary layer, in which a time-averaged eddy viscosity is specified.

In solving the governing equations, most previous models assumed some time-averaged eddy viscosities to make a closure system. Due to the phase variation of physical quantities, this kind of model can not be expected to simulate complicated flow and will lead to incorrect predictions of the mean sediment concentration. A typical example was given in the textbook of Fredose and Deigaard (1992). It is desirable to use an advanced turbulence modeling technique for the simulation of the oscillatory sheet flow in which the eddy viscosity is computed with two-equation model.

This paper presents a complete two-phase flow model to simulate the time varying sediment concentration and turbulent flow kinematics of the wave-induced sheet flow. A single-phase flow model developed by Hagatun and Eidsvik (1986) is extended to a two-phase flow model including the major forces of fluid/particle and particle/particle interactions. The main differences between this paper and Hagatun and Eidsvik's work are: (1) the mobile equivalent sand roughness and the bed concentration are not constant, but functions of the Shields parameter, which varies with time, thus are physically more realistic; (2) the fluid/particle and particle/particle interactions are included in the model and (3) the velocity profile of the two-phase flow is used to calculate the wave friction factor. With these improvements, the present model thus follows more closely the physical situation.

3 Governing equations

The formulation of the problem is based on the continuum assumption and uniform cohesionless sediments. Molecular diffusion and viscous stresses are assumed negligible. The continuity and momentum equations for both sediment phase and fluid phase can be written as follows (Li and Sawamoto, 1995; Dong and Zhang, 1999).

The continuity equations for fluid and sediment phase, respectively, are

$$\frac{\partial(1-c)}{\partial t} + \frac{\partial(1-c)w}{\partial z} = \frac{\partial \overline{c'w'}}{\partial z} \quad (5)$$

$$\frac{\partial c}{\partial t} + \frac{\partial cw_s}{\partial z} = \frac{\partial \overline{c'w'_s}}{\partial z} \quad (6)$$

The momentum equations for fluid phase and sediment phase, respectively, are

$$\frac{\partial \rho_f(1-c)u}{\partial t} = -(1-c) \frac{\partial p}{\partial x} + \frac{\partial \tau_{xz}^f}{\partial z} - f_x \quad (7)$$

$$\frac{\partial \rho_f(1-c)w}{\partial t} = -(1-c) \frac{\partial p}{\partial z} + \frac{\partial \tau_{zz}^f}{\partial z} - f_z - \rho_f(1-c)g \quad (8)$$

$$\frac{\partial \rho_s c u_s}{\partial t} = -c \frac{\partial p}{\partial x} + \frac{\partial \tau_{xz}^s}{\partial z} + \frac{\partial \gamma_{xz}^s}{\partial z} + f_x \quad (9)$$

$$\frac{\partial \rho_s c w_s}{\partial t} = -c \frac{\partial p}{\partial z} + \frac{\partial \tau_{zz}^s}{\partial z} + \frac{\partial \gamma_{zz}^s}{\partial z} + f_x - \rho_s c g \quad (10)$$

where x , z and t denote the Cartesian coordinate system and time, x axis is taken in the horizontal direction and z axis in the vertical direction, c the volumetric concentration of sediment, ν_{ts} the turbulent diffusion coefficient, p the pressure, (u, w) and (u_s, w_s) the x and z components of velocities of the fluid and sediment, respectively, $(\tau_{xz}^f, \tau_{zz}^f)$ and $(\tau_{xz}^s, \tau_{zz}^s)$ the x and z components of the Reynolds stress tensor of the fluid and sediment, γ_{xz}^s and γ_{zz}^s the x and z components of the intergranular stress of the sediment, f_x and f_z the x and z components of the interaction force per unit volume between the fluid and sediment.

Some simplifications are required to capture the main features of the complicated two-phase flow. The convection terms have been neglected in the above equations because the thickness of

the sheet flow layer and its variation in the horizontal direction are very small compared with the wavelength.

To close the system, it is necessary to specify some forcing terms in terms of the primary parameters.

(1) Pressure force

According to the boundary layer theory of the linear wave, the pressure gradient is related to the free stream velocity as follows.

$$\frac{\partial p}{\partial x} = -\rho_f \frac{\partial U}{\partial t} \quad (11)$$

(2) Reynolds stress due to turbulence

Following Kobayashi and Seo (1985), the following simple closure schemes are assumed:

$$\overline{c'w'} \approx \overline{c'w'_s} = -\nu_{ts} \frac{\partial c}{\partial z} \quad (12)$$

$$\overline{u'w'} \approx \overline{u'_s w'_s} = -\nu_{tf} \frac{\partial u}{\partial z} \quad (13)$$

where ν_{tf} is the eddy viscosity. The eddy diffusivity ν_{ts} may be related to ν_{tf} by $\nu_{ts} = \nu_{tf}/\sigma_c$, where σ_c is the Schmidt number. The Reynolds stress is thus given by

$$\frac{\tau_{xz}^f}{\rho_f} = \frac{\tau_{zx}^f}{\rho_f} = -(1-c)\overline{u'w'} = (1-c)\nu_{tf} \frac{\partial u}{\partial z} \quad (14)$$

$$\frac{\tau_{zz}^f}{\rho_f} = (1-c)\nu_{tf} \frac{\partial w}{\partial z} \quad (15)$$

$$\frac{\tau_{xz}^s}{\rho_f} = \frac{\tau_{zx}^s}{\rho_f} = c\nu_{ts} \frac{\partial u_s}{\partial z} \quad (16)$$

$$\frac{\tau_{zz}^s}{\rho_f} = c\nu_{ts} \frac{\partial w_s}{\partial z} \quad (17)$$

(3) Interactive force between the sediment and fluid

The interactive force between the sediment and fluid may be expressed in terms of the sum of the buoyancy and drag, i. e.

$$f_x = \frac{\rho_f}{2} C_D \left(\frac{\pi}{4} D_{50}^2 \right) \frac{c}{\pi D_{50}^3 / 6} u_r \sqrt{u_r^2 + w_r^2} \quad (18)$$

$$f_z = \frac{\rho_f}{2} C_D \left(\frac{\pi}{4} D_{50}^2 \right) \frac{c}{\pi D_{50}^3 / 6} w_r \sqrt{u_r^2 + w_r^2} + \frac{\rho_f}{2} C_L \left(\frac{\pi}{4} D_{50}^2 \right) \frac{c}{\pi D_{50}^3 / 6} |w_r| \frac{\partial u_r}{\partial z} \quad (19)$$

in which C_D and C_L are the drag coefficient and the lift coefficient, respectively, u_r and w_r are the differences between the fluid velocities and the sediment particle velocities:

$$u_r = u - u_s; \quad w_r = w - w_s \quad (20)$$

The lift coefficient C_L is taken to be 4/3 (Dong and Zhang, 1999), while the drag coefficient is estimated using Rubey's formula (Asano, 1990; Dong and Zhang, 1999)

$$C_D = \frac{24\nu}{D_{50}\sqrt{u_r^2 + w_r^2}} + 2 \quad (21)$$

where ν is the kinematic viscosity of water. Although Eq. (21) is only valid for a single particle in homogenous flow, it was still used in the model calculation.

(4) Intergranular stress due to particle/particle interactions

The intergranular stresses result from the momentum transfer from particle to particle in the sediment-laden flow. According to Bagnold (1954), the total shear stress can be expressed as the sum of the shear stress due to the interstitial fluid and the particle/particle interactions. However, Sayed and Savage (1983), and Savag (1984) found that the Bagnold's equations are not entirely satisfactory. Here, we adopt the following empirical formula proposed by Ahilan and Sleath (1987), based on extensive experiments by Savage and Mckeown (1983):

$$\gamma_{xz}^s = 1.2\lambda^2 \rho_f \nu \frac{\partial u_s}{\partial z} \quad (22)$$

where λ is the so-called linear sediment concentration determined by

$$\lambda = \frac{1}{[(c_m/c)^{1/3} - 1]} \quad (23)$$

According to Dong and Zhang (1999), the intergranular stress in the vertical direction is proportional to the shear stress:

$$\gamma_{zz}^s = 1.2\lambda^2 \rho_f \nu \frac{\partial u_s}{\partial z} \cot \phi \quad (24)$$

where ϕ is the friction angle of the sediment and its value is taken to be 40° in the model.

The k- ϵ model is used to simulate flow kinematics and turbulent dynamics in the present study. In the model techniques, the eddy viscosity is related to the turbulent kinetic energy k and the energy dissipation rate ϵ by

$$\nu_{tf} = c_\mu k^2 \epsilon^{-1} \quad (25)$$

The system is thus closed by the transport equations of the Turbulent Kinetic Equation (TKE) and Energy Dissipation Equation (EDE):

$$\frac{\partial k}{\partial t} = \frac{\partial}{\partial z} \left[\frac{\nu_{tf}}{\sigma_k} \frac{\partial k}{\partial z} \right] + P + G - \epsilon \quad (26)$$

$$\frac{\partial \epsilon}{\partial t} = \frac{\partial}{\partial z} \left[\frac{\nu_{tf}}{\sigma_\epsilon} \frac{\partial \epsilon}{\partial z} \right] + [c_1(P + G) - c_2\epsilon] \frac{\epsilon}{k} \quad (27)$$

here the mechanical and buoyant energy production P and G , respectively, are

$$P = \nu_{tf} \left(\frac{\partial u}{\partial z} \right)^2 \quad (28)$$

$$G = g \left(\frac{\rho_s - \rho_f}{\rho_f} \right) \left(\frac{\nu_{tf}}{\sigma_c} \right) \frac{\partial c}{\partial z} \quad (29)$$

In the above equations, the inclusion of the buoyancy term, along with $\partial u/\partial z$ computed from stratified flow equations, should have accounted for the stratification effects of sediment-laden flow. The Schmidt number, σ_c , and the other parameters relating the turbulent diffusion coefficient to eddy viscosity should also depend on vertical density structure. There are numerous

semi-empirical formulations relating the Schmidt number to the gradient Richardson number R_i of stably stratified flow (Nunes Vaz and Simpson, 1994), where R_i is defined as

$$R_i = -\frac{G}{P} = -g \left(\frac{\rho_s - \rho_f}{\rho_f} \right) \left(\frac{\partial u}{\partial z} \right)^{-2} \frac{\partial c}{\partial z} \quad (30)$$

However, none of them has been proved universally satisfactory. Therefore, these parameters are treated as constant coefficients in the present model. Their value are set at $\sigma_k = 1.0$, $\sigma_\varepsilon = 1.3$, $\sigma_c = 1.0$, $c_\mu = 0.99$, $c_1 = 1.44$, and $c_2 = 1.92$ (Justensen, 1988). The k - ε model is limited for the case of high sediment concentration in sheet flows because of large changes of the flow structures. To examine the validated range of the model, a sensitivity test will be made later on to estimate how much the Schmidt number different from 1.0 when different maximum sediment concentrations are used.

4 Boundary conditions

The sediment transport field in the two-phase flow is conventionally divided into two regions: (1) the bed load region where the sediment concentration is high and the sediment particles are mainly supported by the intergranular stresses; (2) the suspended load region where the sediment concentration is small and the Reynolds stress is the predominate force to suspend sediment particles.

In the bed load region, the boundary conditions are

$$u_s = w_s = 0 \quad \text{at } z = eD_{50} - b \quad (31)$$

$$u = w = 0 \quad \text{at } z = z_0 - b \quad (32)$$

$$c = c_b \quad \text{at } z = 0 \quad (33)$$

$$k = \frac{1}{c_\mu} \frac{|\tau_b|}{\rho_f} \quad \text{at } z = z_0 - b \quad (34)$$

$$\varepsilon = \frac{(c_\mu)^{3/4} k^{3/2}}{\kappa z_0} \quad \text{at } z = z_0 - b \quad (35)$$

where $e = 0.8$ is an empirical constant and $z_0 = k_s/30$ is the level of the zero velocity. The equivalent sand roughness k_s is conventionally taken to be $k_s = 2.5D_{50}$ (Einstein and Chien, 1955). However, as mentioned in the previous section, k_s could vary with the thickness of the sediment moving layer in the bed load region. According to Eq. (4), z_0 is related to the Shields parameter:

$$\frac{z_0}{D_{50}} = \frac{k_s}{30D_{50}} = \frac{Y}{6} \quad (36)$$

Based on the experiment of Wilson (1989b), the thickness of the moving layer in the bed load region b , is given by

$$\frac{b}{D_{50}} = 10(Y - Y_{cr}) \quad \text{if } Y > Y_{cr} \quad (37)$$

where Y_{cr} is the critical Shields number, taken to be $Y_{cr} = 0.05$.

In Eq. (33), a reference concentration is prescribed as the bottom boundary condition of sheet flows for equilibrium situations. Apart from using this condition, the net sediment flux is specified at the bed under nonequilibrium conditions (Celik and Rodi, 1988, 1991; Hong and Wang, 2000). The general net flux

boundary condition is given by

$$\frac{v_{if}}{\sigma_c} \frac{\partial c}{\partial z} + w_o c = D - E \quad \text{at } z = 0 \quad (38)$$

in which w_o is the fall velocity in clear water, $D - E$ is the net sediment flux, D the deposition rate and E the entrainment rate. The deposition rate is the product of fall velocity and the bed concentration, i.e. $D = w_o c_b$. According to Celik and Rodi (1988), the entrainment rate may be expressed as

$$E = w_o c_m \quad (39)$$

for a bed covered with loose sediment. The value of maximum concentration c_m is set to be 0.6 as suggested by Li and Sawamoto (1995).

The boundary conditions at the top of the suspended region are

$$u = u_s = U \quad \text{as } z \rightarrow \infty \quad (40)$$

$$w_s = w_o; \quad w = 0 \quad \text{as } z \rightarrow \infty \quad (41)$$

$$\frac{\partial k}{\partial z} = \frac{\partial \varepsilon}{\partial z} = 0 \quad \text{as } z \rightarrow \infty \quad (42)$$

$$c = 0 \quad \text{as } z \rightarrow \infty \quad (43)$$

Figure 2 shows a definition sketch of the boundary conditions specified in the present model.

Based on the experimental results of Wilson (1989a), the upper limit of the suspended region Δ , is estimated by

$$\Delta = \frac{\kappa U_{fm}}{\omega} \quad (44)$$

where U_{fm} is the maximum friction velocity.

Engelund and Fredose (1976) provided a model for calculating c_b from the requirements of momentum transfer to the immobile sand surface, if the transport of a certain probability p of the particles is known. However, due to the uncertainties associated with these empirical parameters, this problem still lacks a completely satisfactory solution, even for the simple case of a steady current. Based on the sensitivity analysis, Engelund and Fredose (1976)

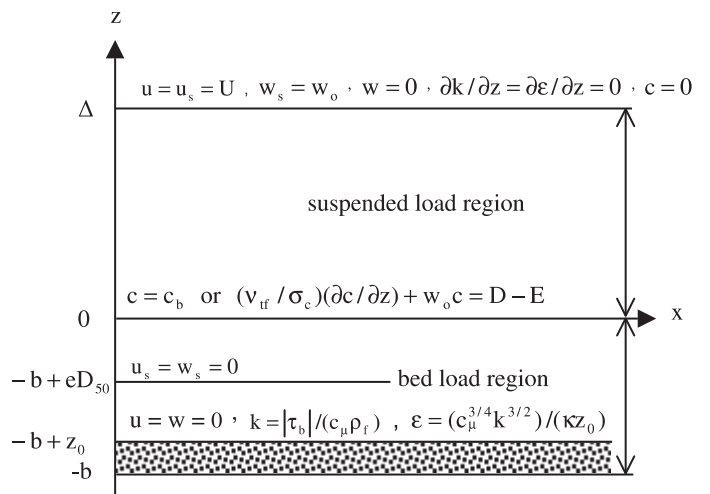


Figure 2 Definition sketch of boundary conditions.

proposed a curve for the calculation of c_b which is approximated by the Shields parameter, that is

$$\begin{aligned} c_b &= 1.30Y^{3.93} & \text{for } 0.01 \leq Y < 0.52 \\ c_b &= -0.15 + 0.59Y - 0.21Y^2 & \text{for } 0.52 \leq Y < 0.99 \\ c_b &= 0.025 + 0.36Y - 0.20Y^2 & \text{for } 0.99 \leq Y < 7 \\ &+ 0.06Y^3 - 0.01Y^4 \end{aligned} \quad (45)$$

Equation (45) does not explicitly take into account the effect of grain-settling. When applied to oscillatory flows, these functions unrealistically give a zero value for the bed concentration during some phases of a wave cycle, when its Shields parameter is smaller than its critical value. To overcome this shortcoming, Fredsoe and Deigaard (1992) proposed a modified equation:

$$c_b = \max\{c_b(Y), c(b + w_o \Delta t, t - \Delta t)\} \quad (46)$$

The bottom shear stress can be obtained by means of the following equation

$$\frac{\tau_b}{\rho_f} = \nu_{tf} \left. \frac{\partial u}{\partial z} \right|_{z=z_0} \quad (47)$$

According to Jonsson and Carlsen (1976), the wave friction factor can be defined as

$$\frac{\tau_{bm}}{\rho_f} = \frac{f_w}{2} U_m^2 \quad (48)$$

where τ_{bm} is the maximum value of τ_b . If we expand the shear stress term of Eq. (2) in a Fourier Sine series and keep only the first term, Eq. (2) is rewritten as (Dean and Dalrymple, 1984)

$$\frac{\tau_b}{\rho_f} = \frac{8}{3\pi} C_f U_m^2 \sin \omega t \quad (49)$$

Taking the maximum value of Eq. (49) and comparing it with Eq. (48), we get the following expression:

$$f_w = \frac{16}{3\pi} C_f \quad (50)$$

The wave friction factor, which differs from rough wall law, could be estimated by the velocity gradient of the mean motion by using Eqs. (4), (36) and (47). Wilson (1989b) assumed a logarithmic velocity profile in the oscillatory flow to estimate the wave friction. His result is expressed as

$$X = \frac{3}{20\pi} \sqrt{\frac{2}{C_f}} \exp \left[-0.4 \sqrt{\frac{2}{C_f}} \right] \quad (51)$$

where

$$X = \frac{\rho_f A_b}{(\rho_s - \rho_f) g T^2} \quad (52)$$

Equation (51) indicates that the wave friction factor is related to the dimensionless parameter X , which shares the relative roughness A_b/k_s and relates more readily to the wave steepness (Hsu and Ou, 1994). On the other hand, substituting Eqs. (1), (2) and (3) into Eq. (36) yields

$$\frac{z_0}{A_b} = \frac{2\pi^2}{3} X C_f |\sin \omega t| \sin \omega t \quad (53)$$

Thus the wave friction factor can be related to the parameter X from the present model formulation without assuming the logarithmic profile.

5 Numerical procedure

For computational convenience, the physical variables in the governing equations are first non-dimensionalized as follows,

$$z^* = \frac{z}{A_b}, \quad z_0^* = \frac{z_0}{A_b}, \quad \ell^* = \frac{\ell}{A_b} \quad (54)$$

$$\begin{aligned} U^* &= \frac{U}{A_b \omega}, \quad u^* = \frac{u}{A_b \omega}, \quad u_s^* = \frac{u_s}{A_b \omega}, \\ w^* &= \frac{w}{A_b \omega}, \quad w_s^* = \frac{w_s}{A_b \omega} \end{aligned} \quad (55)$$

$$\nu_{tf}^* = \frac{\nu_{tf}}{A_b^2 \omega}, \quad \nu_{ts}^* = \frac{\nu_{ts}}{A_b^2 \omega}, \quad k^* = \frac{k}{A_b^2 \omega^2}, \quad \varepsilon^* = \frac{\varepsilon}{A_b^2 \omega^3} \quad (56)$$

$$t^* = \omega t \quad (57)$$

$$\rho_s^* = \frac{\rho_s}{\rho_f} \quad (58)$$

$$\begin{aligned} \tau_{xz}^{f*} &= \frac{\tau_{xz}^f}{\rho_f A_b^2 \omega^2}, \quad \tau_{xz}^{s*} = \frac{\tau_{xz}^s}{\rho_f A_b^2 \omega^2}, \\ \gamma_{xz}^{s*} &= \frac{\gamma_{xz}^s}{\rho_f A_b^2 \omega^2}, \quad f_{x(z)}^* = \frac{f_{x(z)}}{\rho_f A_b \omega^2} \end{aligned} \quad (59)$$

Given boundary conditions, the system of discretized governing equations can be solved by an iteration process. The standard discretized equations can be derived using the finite volume method. The detailed formulations may be found in Hsu and Lin (1998). The relaxation method of Patankar (1980) is used to speed up the numerical convergence. The representation of the discretized equations may be written in the general matrix form

$$A(I)X(I) = B(I)X(I+1) + C(I)X(I-1) + D(I) \quad (60)$$

where $B(I)$ and $C(I)$ are coefficient matrices, the matrix $X(I)$ represents the corresponding terms such as mean flow velocity (u, w), velocities of sediment particles (u_s, w_s), turbulent kinetic energy k , energy dissipation rate ε and sediment concentration c . $A(I)$ and $D(I)$ are the modified values of the coefficient matrix $a(I)$ and $d(I)$, respectively, and are written as

$$A(I) = \frac{a(I)}{\alpha_x} \quad (61)$$

$$D(I) = d(I) + (1 - \alpha_x) \frac{a(I)}{\alpha_x} X^0(I) \quad (62)$$

where $X^0(I)$ is the value obtained from the previous iteration and α_x is the relaxation coefficient taken to be 0.85.

To achieve a more detailed description of the mechanics of the boundary layer for a two-phase flow, the vertical grid spacing is specified with a cubic scale that has finer grid near the bottom,

$$z^*(I) = H^* \left(\frac{I-1}{N-1} \right)^3 \quad (63)$$

where $H^* = \Delta/A_b$ is the height of the computational domain and N the total number of grid points. In this study, we set $N = 100$, $\Delta t = 2\pi/240$. A relative error of the iteration is defined as

$$E_r = \left| \frac{[X^{K+1}(I) - X^K(I)]}{X^K(I)} \right| \quad (64)$$

where K denotes the number of iterations. The magnitude of E_r is set to be 10^{-3} for the present study. It is found that the

240 time steps in one wave period is a reasonable number. The parameters and convergence criteria used in this study are based on a compromise between accuracy and speed of computation. Numerical experiments show that the required precision for the iteration procedure can be reached after 6 to 12 wave periods.

6 Model validation

The present model is validated by comparing model results with measurements. The experiments performed by Horikawa *et al.* (1982) and Staub *et al.* (1984) provided the data for comparisons. The determination of the thickness of the sediment moving layer is important, since it defines the upper and lower boundary in the whole computational domain. The upper and lower limits of the sediment moving layer in the suspended region and bed load region (Fig. 2) are estimated by Eqs. (36) and (43), respectively. These empirical formula were validated against the experimental data of Horikawa *et al.* (1982). Figure 3 shows a comparison of the phase variation of the upper and lower elevations of sediment moving layer during a half wave cycle. It can be seen that the calculations are in good agreement with the measurements.

To calculate the phase-varying sediment concentration, the continuity equations are solved coupled with the momentum and transport equations for TKE and EDE. The experimental results of the instantaneous sediment concentration in Fig. 4 were conducted by Staub *et al.* (1984) with the input parameters: $U_m = 1.2$ m/s, $T = 9.1$ s and $D_{50} = 0.19$ mm. The measurement is made at 1.8 cm above the bottom. The figure shows that the present model provides better estimates than those of Hagatun

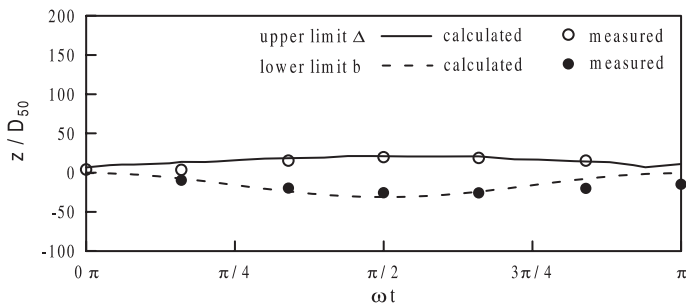


Figure 3 Phase variations of sediment moving layer.

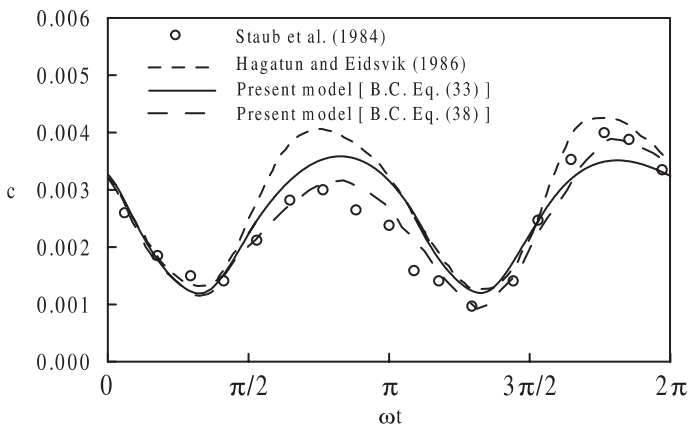


Figure 4 Computed and measured phase variations of sediment concentration at $z = 1.8 \times 10^{-2}$ m.

and Eidsvik's model during the phase from $\pi/2$ to π , however the difference is marginal for the other phases. The vertical distribution of sediment concentration is mainly dependent on the bed concentration c_b . Equation (45) relates the value of c_b to the Shields parameter Y . In Hagatun and Eidsvik's model, c_b is approximated by $c_b = 0.3$ for $Y > 0.75$. This prescription usually leads to a higher value of c_b for $0.75 < Y < 0.99$, resulting in an over-estimate of the sediment concentration. Furthermore, the sand roughness and the thickness of the sediment moving layer b are both dependent on the Shields parameter Y , but these variables are set to be constant values ($z_0 = 0.08D_{50}$ and $b = 2D_{50}$) in Hagatun and Eidsvik's model. Their boundary conditions may result in inaccurate concentrations.

The comparisons between the computed mean sediment concentration from the present model, Hagatun and Eidsvik's model, and the experimental data of Horikawa *et al.* (1982) are shown in Fig. 5. It is found that the present model matches better with the experimental data, with the exception of case 2, for which Hagatun and Eidsvik's model give a similar results. Figure 6 shows the comparisons between the computed profile of mean sediment concentration with the experimental data of Staub *et al.* (1984). The computational conditions are the same as those of Fig. 4. The circles in the figure are the experimental data with their confidence ranges shown by the vertical lines. It shows that the mean sediment concentration computed by the present model agrees reasonably well in the range with the experimental data, while Hagatun and Eidsvik's (1986) model apparently over-predicts at $1 \text{ cm} < z < 2 \text{ cm}$, but both models predict a slightly higher concentration than experimental data away from the bed ($z > 2 \text{ cm}$). This is consistent with Fig. 4, which shows that their predicted instantaneous concentration is higher than the experimental data at $z = 1.8 \text{ cm}$.

The key feature of wave-induced sheet flows is interactions between fluid motion and sediments. The velocity distribution of the sheet flow is affected by the presence of sediment particles, and the velocity defects increase with the sediment concentration. Figure 7 is a comparison of the velocity profiles from the models and the experimental data of Horikawa *et al.* (1982).

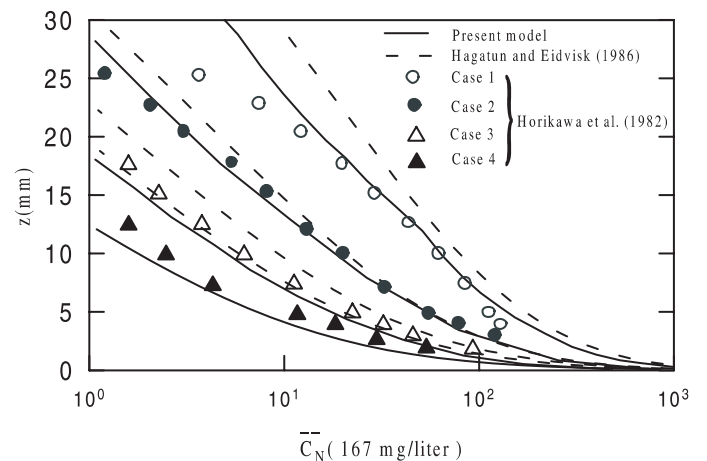


Figure 5 Computed and measured vertical variations of mean sediment concentrations. $A_b = 0.72$, $T = 0.36$ s; 4.2 s; 4.8 s; 5.4 s, $D_{50} = 0.2$ mm, $w_0 = 0.026$ m/s.

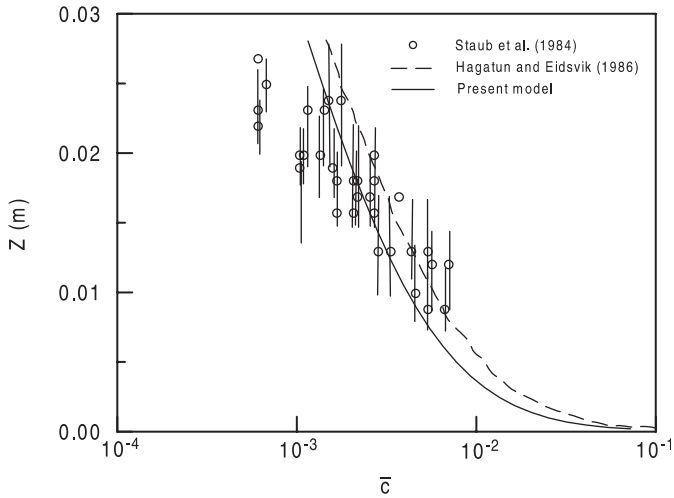


Figure 6 Computed and measured vertical variations of mean sediment concentrations.

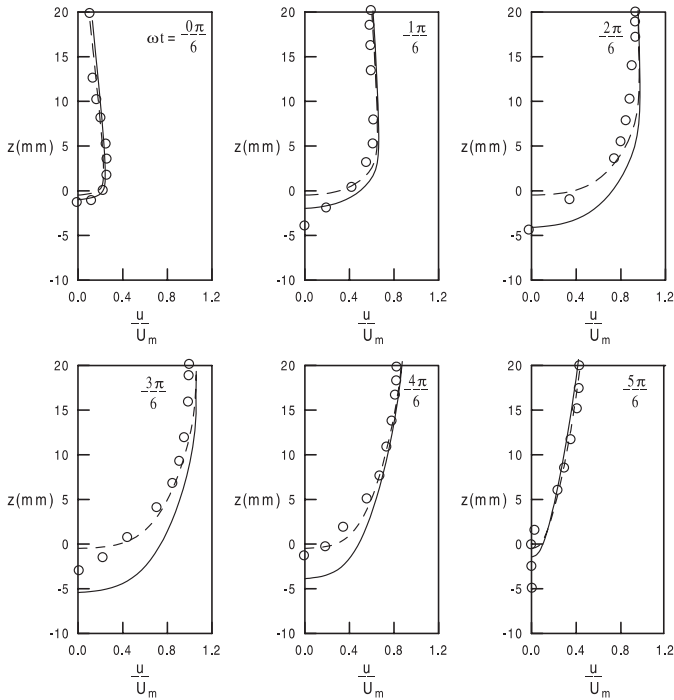


Figure 7 Computed and measured phase variations of the velocity profiles in the two-phase flow field. \circ : Experiments from Horikawa *et al.* (1982); —: present model; - - -: Hagatun and Eidsvik (1986).

The calculated velocities from both models agree fairly with the experimental measurement at all phases. For a quantification of the differences between the present and Hagatun and Eidsvik’s model, we define a relative error index E_r :

$$E_r = \frac{2}{T} \frac{1}{N} \sum_{t=0}^{\pi} \sum_{n=1}^N \left| \frac{\tilde{H}_n^t - H_n^t}{H_n^t} \right| \quad (65)$$

where N denotes the total number of the measuring points, H_n^t is the measured value and \tilde{H}_n^t is the calculated value from the model. Table 1 presents the relative errors between the prediction and measurement. It is evident that present model provides a more accurate sediment concentration field, while the two models performances are about the same in predicting the velocity profile.

Table 1 Comparison of relative error E_r between predictions and measurements (%).

Models	Velocity profile	Sediment concentration	
		Mean	Phase variation
Hagatun and Eidsvik (1986)	21.5	58.8	18.8
Present model	22.8	23.7	8.8

The experimental data used to calculate E_r are from Horikawa *et al.* (1982) and Staub *et al.* (1984).

7 Sensitivity analysis

Possible causes may result in the differences of model results include the following: (1) the influence of the turbulent diffusion coefficient; (2) the specified boundary condition of the sediment concentration near the bed for equilibrium and nonequilibrium situations and (3) the determination of the thickness of sediment moving layer in the bed load region. A sensitivity analysis was carried out to justify model performance.

In Eqs. (26) and (27), the $k-\epsilon$ model for two phase flow is used to close the turbulent system. The buoyant energy production term, G , is included in both equations to account for the sediment effects on turbulence. It is difficult to justify that the present model is still valid under high sediment concentration in sheet flows. For the purpose of illustrating the properties of the model, a sensitivity analysis is made to examine how much the Schmidt number σ_c different from 1.0 which is traditionally accepted for other flows with different bed concentrations. The results are presented in Fig. 8(a), showing that an increase of bed concentration produces a little bit larger Schmidt number, but the magnitude of increase is within 60% as $c_m < 0.6$. The influence of the Schmidt number on model results is studied by applying different Schmidt numbers ranging from 1.0 to 1.7. The relative errors of computed and measured concentrations are shown in Fig. 8(b). The input parameters are the same as those in Fig. 4. It is seen that there is no clear difference between computed and measure results for different values of σ_c . From the sensitivity analysis, we conclude that the present $k-\epsilon$ model in two phase flow is still proper when $c_m < 0.6$.

To understand the influence of the specified bottom boundary conditions in Eqs. (33) and (38) on the model results, two different calculations were run by applying these two boundary conditions. The results of the computations are presented in Fig. 4. It is noted that the net sediment flux boundary condition for nonequilibrium situations gives a better agreement between computed and measured sediment concentration than that for equilibrium situations. This seems logical because it is physically more realistic to specify the net sediment flux at the bottom boundary. Because of the complexity of two phase flow, these two boundary conditions should be further justified through available data.

A sensitivity analysis was also performed to evaluate the effects of different choices of the thickness of the sediment moving layer B on the predicted horizontal flow velocity, which B is an

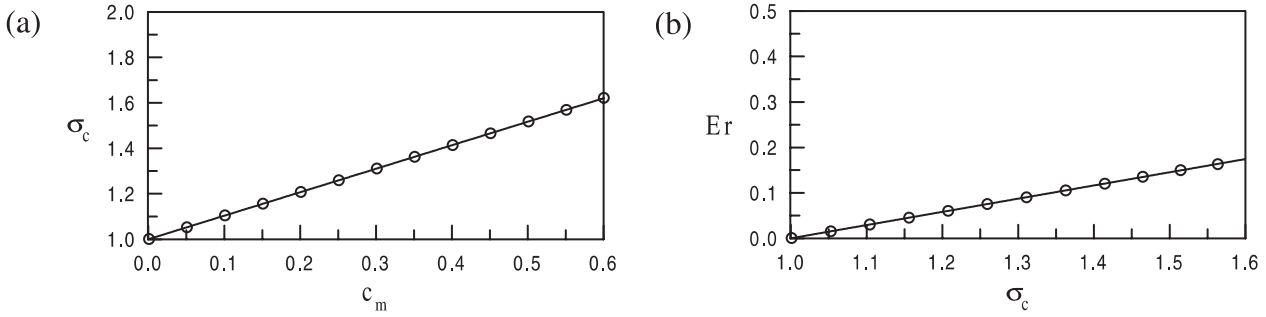


Figure 8 The sensitivity analysis. (a) the Schmidt number σ_c versus the maximum bed concentration; (b) the relative error versus the Schmidt number.

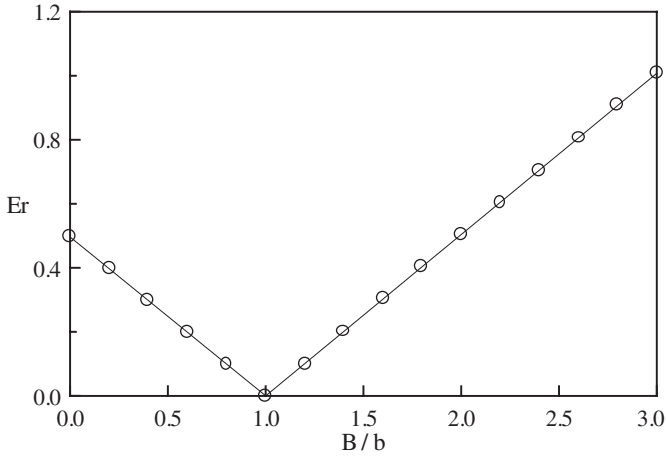


Figure 9 The sensitivity analysis of mean flow velocity, for different moving layer thickness in bed load region.

assumed thickness of the moving layer. Flows that are representative for oceanic waves are simulated for the situation $U_m = 1$ m/s, $T = 10$ s, $D_{50} = 2 \times 10^{-4}$ m. We can see from Fig. 9 that the value of Er strongly depends on the thickness of the shear layer, implying that the determination of the thickness of the sediment moving layer in the bed load region is of great importance for predictions of flow kinematics and sediment concentrations.

8 Results and discussion

Figure 10 shows the calculated horizontal velocities u and u_s of the fluid and sediment at different phases. In the bed load region, the sediment transport velocities are extremely small because of the large intergranular stress. At the upper part of the suspended region, the velocities follow the free stream velocity, since the sediment concentration there is low. In the middle part of the suspended region, a phase precedence over the free stream velocity is observed.

The characteristics of the boundary layer of the two-phase flow are investigated through numerical computations. Figure 11 shows the phase variation of the horizontal mean velocity profiles, with and without sediment transport, with $A_b/k_s = 3183$. It shows that the velocity is higher in the flow without sediment transport, i.e. the presence of suspended sediments retards the entire mean velocity profile.

The sediment content affects the other physical quantities too, such as the turbulent kinetic energy, eddy viscosity and the

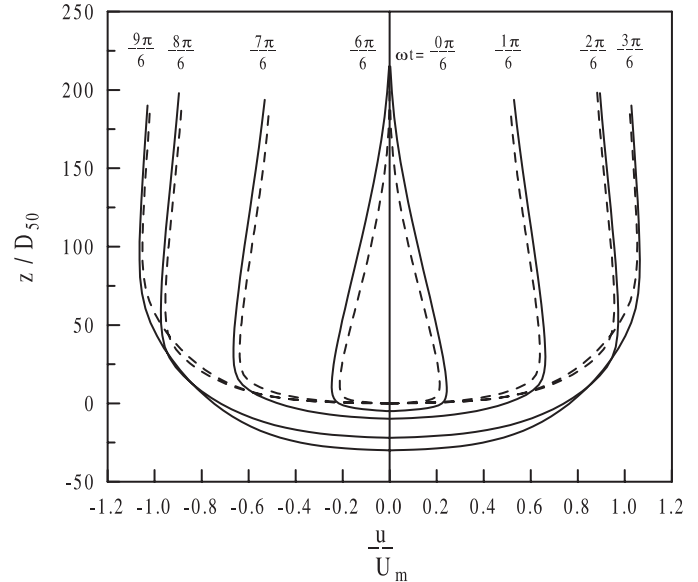


Figure 10 Phase variation of fluid and sediment velocities. —: fluid; ---: sediment.

Reynold stress. A comparison of these quantities, with and without suspended sediments, are illustrated in Fig. 12. It is observed that these corresponding quantities are lower with suspended sediments. This indicates that the turbulence kinetic energy decreases due to the presence of sediment particles. In other words, the energy required to support suspended load mainly comes from the turbulent kinetic energy rather than the mean flow energy. It is also noted in Fig. 11 that the velocity gradient in the sediment-laden flow increases, in response to reduce a larger value of the eddy viscosity.

The relation between the wave friction factor, f_w , and the parameter, X , of sheet flows is presented in Fig. 13. It is noted that the friction coefficient increases with the increase of X . Hsu and Ou's (1994) and Wilson's (1989b) empirical formulas are also presented in the figure. It was found that the predicted wave friction factor from the present model is lower than that of the previous models. This result is due to the fact that the decreased bed shear stress in the present model produces a lower value of the wave friction factor. The relationship between f_w and X obtained from the present model is linear in the logarithmic coordinates, and can be represented by a regression equation as

$$f_w = 0.12X^{0.42} \quad (66)$$

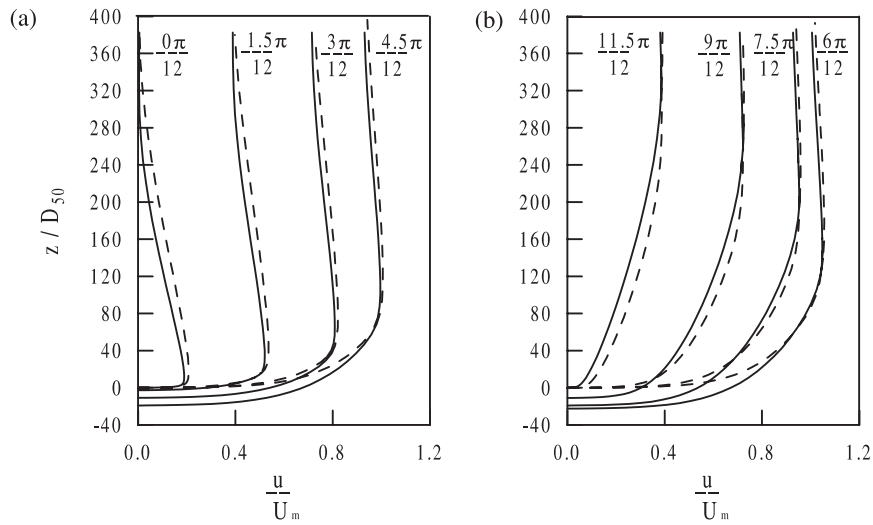


Figure 11 A comparison of horizontal mean velocity profile with and without suspended sediments. (a) Accelerating phase, (b) decelerating phase. —: $c \neq 0$; ---: $c = 0$.

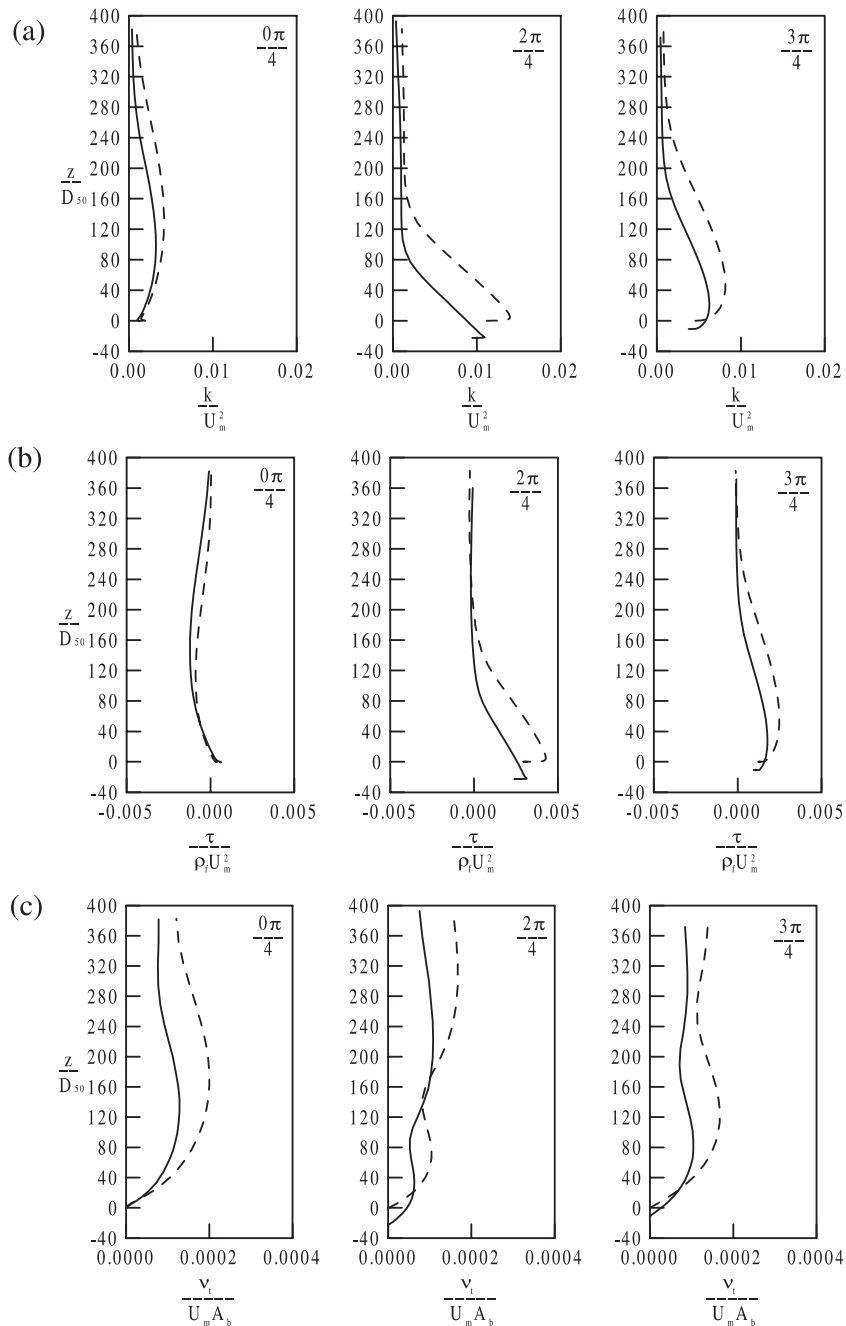


Figure 12 A comparison of turbulent quantities for different phase with and without suspended sediments. (a) Kinetic energy, (b) Reynolds stress, (c) eddy viscosity. —: $c \neq 0$; ---: $c = 0$.

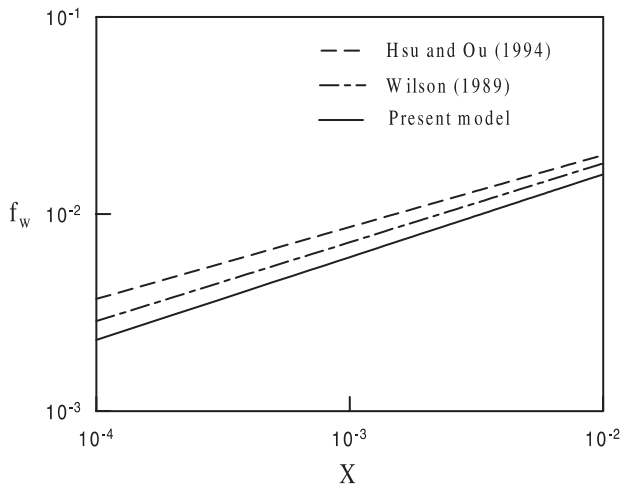


Figure 13 Wave friction factor for wave-induced sheet flow.

9 Summary and conclusions

A complete two-phase flow model for describing the flow kinematics, sediment concentrations and bed shear stresses under wave-induced sheet flow conditions has been developed. A k - ϵ turbulence closure model is employed for the simulation of the complicated two-phase flow. The major forcing such as the fluid/particle and particle/particle interactions and the Reynolds stresses are included in the model. Modifying the boundary conditions of the existing two-phase flow model, the present model specifies the equivalent sand roughness and the bed concentration as functions of the time dependent Shields parameters for equilibrium situations. An alternative to specify the net sediment flux at the bottom boundary for nonequilibrium sediment transport is also applied. The comparison with the available experimental data demonstrates that the model is capable of describing flow kinematics and sediment concentrations in the wave-induced sheet flow.

The wave friction factor of the two-phase flow is obtained from the conventional definition of the bed shear stress. The result is similar to that reported by Wilson (1989b) in the way by which the friction factor depends on a new parameter X . It shares the relative roughness and relates to the wave steepness. The wave friction factor estimated from the present model is lower than those obtained by previous single-phase flow models.

The present model shows that the velocity is retarded by the presence of sediment. The analysis of the effects of sediment suspension on turbulent kinetic energy, Reynolds stress and turbulent eddy viscosity shows that (1) sediment suspension reduces the turbulent kinetic energy; (2) sediment suspension reduces the Reynolds stress and (3) sediment suspension reduces a turbulent eddy viscosity which corresponds to an increased velocity gradient.

The present numerical model is based on more rigorous theoretical formulations than most of the previous models. However, the empirical formulae used for the modeling of fluid/particle and particle/particle interactions are related to empirical coefficients which were evaluated from limited experimental data. These

coefficients should be further examined through more available data to improve predictions.

Acknowledgement

This research is supported by the National Science Council of Taiwan under the grant of NSC-85-2611-E-006-013.

References

- ADAMS, C.E. and WETHERLY, G.L. (1981). "Some Effects of Suspended Sediment Stratification on an Oceanic Bottom Boundary Layer", *J. Geophys. Res.*, 86, 4161–4172.
- AHILAN, R.V. and SLEATH, J.F.A. (1987). "Sediment Transport in Oscillatory Flow Over Flat Bed", *J. Hydraul. Engrg.*, 113(3), 308–322.
- ASANO, T. (1990). "Two-phase Flow Model on Oscillatory Sheet-flow", *Proc. 22nd Conf. Coastal Engrg. ASCE*, 2372–2384.
- BAGNOLD, R.A. (1954). "Experiments on a Gravity Free Dispersion of Large Solid Spheres in a Newtonian Fluid Under Shear", *Proc. Royal Soc.*, A255, 49–63.
- BAKKER, W.T. (1974). "Sand Concentration in an Oscillatory Flow", *Proc. 14th Conf. Coastal Engrg. ASCE*, Copenhagen, 1129–1148.
- CELIK, I. and RODI W. (1988). "Modeling Suspended Sediment Transport in Nonequilibrium Situations", *J. Hydr. Engrg. ASCE*, 114(10), 1157–1191.
- CELIK, I. and RODI. W. (1991). "Suspended Sediment-transport Capacity for Open Channel Flow", *J. Hydr. Engrg.*, 117(2), 191–204.
- COLEMAN, N.L. (1980). "Velocity Profiles with Suspended Sediment", *J. Hydr. Res.*, 19, 211–229.
- DEAN, R.G. and DARYMPLE, R.A. (1984). *Water Wave Mechanics for Engineers and Scientists*. Prentice-Hall of Southeast Asia Pte. Ltd., Singapore.
- DONG, P. and ZHANG, K. (1999). "Two-phase Flow Modeling of Sediment Motions in Oscillatory Sheet Flow", *Coastal Engrg.*, 36, 87–109.
- EINSTEIN, H.A. and CHIEN, N. (1955). *Effects of Heavy Sediment Concentration near the Bed on Velocity and Sediment Distribution*. University of California Institute of Engineering Research, MRD Sediment Series Report No. 8.
- ENGELUND, F. and FREDSOE, J. (1976). "A Sediment Transport Model for Straight Alluvial Channels", *Nordic Hydrolog.*, 7, 293–306.
- FREDSOE, J., ANDERSEN, O.H. and STEEN, S. (1985). "Distribution of Suspended Sediment in Large Waves", *J. Waterways, Port, Coastal and Ocean Engrg. ASCE*, 111(6), 1041–1059.
- FREDSOE, J. and DEIGAARD, R. (1992). *Mechanics of Coastal Sediment Transport*. World Scientific Publishing Co. Pte. Ltd., Singapore, p. 369.

15. GOTOH, H. and SAKAI, T. (1997). "Numerical Simulation of Sheet-flow as Granular Material", *J. Waterways, Port, Coastal and Ocean Engrg.* ASCE, 123(6), 329–336.
16. GRANT, W.D. and MADSEN, O.S. (1982). "Movable Bed Roughness in Unsteady Oscillatory Flow", *J. Geophys. Res.*, 87, 469–481.
17. HAGATUN, K. and EIDSVIK, K.J. (1986). "Oscillatory Turbulent Boundary Layers with Suspended Sediments", *J. Geophys. Res.*, 91(C11), 13,045–13,055.
18. HONG, W.F. and WANG G.Q. (2000). "Three-dimensional Mathematical Model of Suspended-sediment Transport", *J. Hydr. Engrg.* ASCE, 126(8), 578–591.
19. HORIKAWA, K., WATANABE, A. and KATORI, S. (1982). "Sediment Transport under Sheet Flow Conditions", *Proc. 18th Conf. Coastal Engrg.* ASCE, Capetown, 1335–1352.
20. HSU, T.W. and OU, S.H. (1994). "Mean Sediment Concentration and Turbulent Boundary Layer of Wave-induced Sheet Flow", *J. Hydr. Res.*, 32, 675–687.
21. HSU, T.W. and LIN, H.Y. (1998). "Applications of a Model to Instantaneous Sediment Concentration and Turbulent Boundary Layers of Wave-induced Sheet Flows", *Proc. 7th Int. Symposium on Flow Modeling and Turbulence Measurements*, Taiwan, 27–38.
22. JUSTESEN, P. (1988). "Prediction of Turbulent Oscillatory Flow over Rough Beds", *Coastal Engrg.*, 12, 257–284.
23. JONSSON, I.G. and CARLSEN, N.A. (1976). "Experimental and Theoretical Investigation in an Oscillatory Turbulent Boundary Layer", *J. Hydr. Res.*, 14(1), 45–60.
24. KOBAYASHI, N. and SEO, N.J. (1985). "Fluid and Sediment Interaction over a Plan Bed", *J. Hydr. Engrg.* ASCE, 111(6), 903–921.
25. LI, L. and SAWAMOTO, M. (1995). "Multi-phase Model on Sediment Transport in Sheet Flow Regime Under Oscillatory Flow", *Coastal Engrg. Japan*, 38, 157–178.
26. NADAOKA, K. and YAGI, H. (1990). "Single-phase Fluid Modeling of Sheet-flow Toward the Development of Numerical Mobile Bed", *Proc. 22th Int. Conf. Coastal Engrg.* ASCE, 2346–2359.
27. NUNES VAZ, R.A. and SIMPSON, J.H. (1994). "Turbulence Closure Modeling of Estuarine Stratification", *J. Geophys. Res.*, 99(C8), 16143–16160.
28. ONO, M., DEUUCHI, I. and SAWARAGI, T. (1996). "Numerical Modeling of Sediment Transport for Various Mode", *Proc. 25th Conf. Coastal Engrg.* ASCE, 3888–3900.
29. PATANKAR, S. (1980). *Numerical Heat Transfer and Fluid Flow*. Hemisphere, Washington D.C., p. 197.
30. RIBBERINK, J.S. and AL-SALEM, A.A. (1995). "Sheet Flow and Suspension of Sand in Oscillatory Boundary Layers", *Coastal Engrg.*, 25, 205–225.
31. SAVAGE, S.B. (1984). "The Mechanics of Rapid Granular Flows", *Adv. Appl. Mech.*, 24, 289–367.
32. SAVAGE, S.B. and MCKEOWN, S. (1983). "Shear Stresses Developed During Rapid Shear of Concentrated Suspensions of Large Spherical Particles Between Concentric Cylinders", *J. Fluid Mech.*, 127, 453–472.
33. SAYED, M. and SAVAGE, S.B. (1983). "Rapid Gravity Flow of Cohesionless Granular Materials Down Inclined Chutes", *J. Appl. Math. Phys.*, 34, 84–100.
34. SMITH, J.D. and MCLEAN, S.R. (1977). *Boundary Layer Adjustments to Bottom Topography and Suspended in Bottom Turbulence*, ed. Nihoul, Elsevier, New York, 123–151.
35. STAUB, C., JONSSON, I.G. and SVENDSEN, I.A. (1984). "Variation of Sediment Suspension in Oscillatory Flow", *Proc. 19th Conf. Coastal Engrg.* ASCE, Houston, 2310–2321.
36. VANONI, V.A. (1946). "Transportation of Suspended Sediment by Water", *Trans. ASCE*, 111, 67–133.
37. VONGVISESSOMJAI, S. (1986). "Profile of Suspended Sediment Due to Wave Action", *J. Waterways, Port, Coastal and Ocean Engrg.*, 112(1), 35–53.
38. WILSON, K.C. (1989a). "Mobile-bed Friction at High Shear Stress", *J. Hydr. Engrg.* ASCE, 115(6), 825–830.
39. WILSON, K.C. (1989b). "Friction of Wave-induced Sheet Flow", *Coastal Engrg.*, 12, 371–379.
40. WILSON, K.C., ANDERSEN, J.S. and SHAW, J.K. (1995). "Effects of Wave Asymmetry on Sheet Flow", *Coastal Engrg.*, 25, 191–204.